Reconstruction of Nonlinear Contact Forces Beyond Limited Measurement Locations Using an SVD Modal Filtering Approach

Patrick Logan[1], Deborah Fowler, Peter Avitabile
University of Massachusetts Lowell
Structural Dynamics and Acoustic Systems Laboratory
1 University Avenue
Lowell, MA 01854

Jacob Dodson
Air Force Research Laboratory
306 W. Eglin Blvd
Eglin AFB, FL 32542

ABSTRACT

Inverse processes are often necessary to assess operating loads, especially when the loads are difficult to measure directly. Reconstruction is generally performed from vibration response data and some form of system model. Where some mismatch in dynamic behavior exists between the model and the real system, the estimated loads may be distorted. However, if the changes in system behavior are of interest, then those changes may be characterized through force reconstruction as equivalent loads acting in conjunction with the original external inputs. These system changes may be linear in nature, but the concept may be extended to nonlinear behavior, including intermittent contact between components.

A modal based methodology for localization and reconstruction of inputs at potentially unmeasured locations is applied to the characterization of local system changes through their equivalent loading. An experimental validation study is presented using a multi-plate structure subject to impact loading and an unmodeled contact condition.

KEYWORDS: force reconstruction, input localization, modal filters, equivalent loading, contact nonlinearity

INTRODUCTION

Where a system is subject to harsh dynamic environments, occurrences of intermittent contact between system components can result in impulsive, high amplitude forces at the contact interfaces. When brittle or fragile components are involved, the resulting contact forces may induce damage. Therefore, identification and characterization of interfacial contact is desirable from a structural health monitoring (SHM) perspective. However, in lieu of the traditional SHM focus on damage detection [1-4], the interest is not in identification of actual damage, but the contact forces preceding potential damage. Where real response data and a representative system model are available, force reconstruction methodologies may be used to identify and reconstruct the forces attributable to the contact nonlinearities.

Early work by Zhang, Allemang and Brown [5] employed a singular value decomposition of modal force estimates to localize inputs to sensor locations. The technique was later extended by Logan and Avitabile [6], to permit localization and subsequent reconstruction of hammer impacts at unmeasured locations of a free-free beam for a linear system. Logan, Fowler and Avitabile [7] further extended the methodology to localize and reconstruct the contact chatter resulting from a nonlinear gap spring element on a multi-component mass-spring-dashpot system.

This paper provides an overview of the relevant force reconstruction theory, followed by experimental validation using a multi-plate structure subject to intermittent contact with an external thumper. The methodology is applied to localize the thumper and reconstruct the associated contact chatter from a purely linear modal representation of the system, with no knowledge of the contact or the second component.

THEORETICAL BACKGROUND

The response of a linear system $X \in \mathbb{C}^{o \times 1}$, at some set of o observed degrees of freedom (DOF), to forces, $F \in \mathbb{C}^{i \times 1}$, acting over some set of i input degrees of freedom, can be expressed as

$$X(j\omega) = \left[H(j\omega)\right] F(j\omega) \tag{1}$$

where the system is characterized by a matrix of frequency response functions, $[H] \in \mathbb{C}^{o \times i}$, between the o observed DOF and the i input DOF, for any spectral line having frequency $j\omega$. The input force can be reconstructed by an inversion of the FRF matrix as

$$F(j\omega) = \left[H(j\omega)\right]^{\dagger} X(j\omega) \tag{2}$$

where the superscript $\dagger$ represents the pseudo-inverse, or the standard inverse where the matrix is square and nonsingular.

The inversion represented within (2) suffers from ill-conditioning and is greatly affected by perturbation of the data. Alternatively, limitation to i input DOFs and o response DOFs over m modes permits the FRF matrix to be written as

$$\left[H(j\omega)\right] = \left[U_{RESPONSE}\right] \left[\bar{H}(j\omega)\right] \left[U_{INPUT}\right]^{T} + \left[R(j\omega)\right] \tag{3}$$

where $[U_{RESPONSE}] \in \mathbb{R}^{o \times m}$ denotes the matrix of mode shape coefficients (scaled to unit modal mass) associated with the selected modes and response DOFs, $[\bar{H}] \in \mathbb{C}^{m \times m}$ is a square diagonal matrix of FRFs for the uncoupled modal oscillators, $[U_{INPUT}] \in \mathbb{R}^{i \times m}$ is the matrix of mode shape coefficients for the input DOFs, and $[R] \in \mathbb{C}^{o \times i}$, is a matrix of residual terms not represented in the retained modes. The matrix of residuals may be considered negligible when the physical response is comprised mostly of the response of the m retained modes. Where acceleration measurements are employed, the FRF for the kth modal oscillator is obtained from the natural frequency, $\omega_{n,}$ and modal damping, ζ, as

$$\bar{H}_{k,k}(j\omega) = \frac{-\omega^2}{\omega_{n,k}^2 - \omega^2 + 2\zeta_k \omega_{n,k} j\omega} \tag{4}$$

Modal response coordinates $p \in \mathbb{C}^{m \times 1}$ may be estimated from the physical coordinates as

$$p(j\omega) = \left[U_{RESPONSE}\right]^{\dagger} X(j\omega) \tag{5}$$

where the pseudo-inverse of the modal coefficient matrix $[U_{RESPONSE}]$ may be considered as a set of modal filters.

Modal domain force, $\bar{F} \in \mathbb{C}^{m \times 1}$, may be estimated from modal coordinates as

$$\bar{F}(j\omega) = \left[\bar{H}(j\omega)\right]^{-1} p(j\omega) \tag{6}$$

From basic modal theory, modal forces are related to physical forces by the modal coefficients of the associated physical DOFs as

$$\bar{F}(j\omega) = \left[U_{INPUT}\right]^{T} F(j\omega) \tag{7}$$

Once physical input DOFs are identified, and, assuming that the number of physical inputs is less than or equal to the number of modes used, the estimation process is completed by transforming the modal forces to physical space as

$$F(j\omega) = [U_{INPUT}]^{-T} \bar{F}(j\omega) \tag{8}$$

where the superscript -T indicates the pseudo-inverse of the transpose. However, identification of the sources must be performed prior to transformation back to physical space. To characterize the sources, an m-by-q matrix of the m modal forces may be assembled over q spectral lines (with $m \leq q$) and decomposed via singular value decomposition (SVD) as

$$[\Upsilon][\Sigma][V]^h = \begin{bmatrix} \bar{F}(j\omega_1) & \bar{F}(j\omega_2) & \cdots & \bar{F}(j\omega_q) \end{bmatrix} \tag{9}$$

where $[\Sigma] \in \mathbb{R}^{m \times q}$ is a diagonal matrix of singular values, $[V] \in \mathbb{C}^{q \times q}$ is a unitary set of basis vectors related to frequency content, $[\Upsilon] \in \mathbb{C}^{m \times m}$ is a set of basis vectors related to the modal coefficients of the input DOFs and the superscript h denotes the conjugate transpose operator. The singular values are representative of the independent force components, and interrogation of the singular values permits identification of the number of independent sources. Where some number of singular values are negligible, omission of the negligible singular values and associated singular vectors does not significantly alter the modal force matrix. Therefore, the modal force matrix may be approximated solely by the a ($a < m$) non-negligible singular values and the associated basis vectors as

$$\left[\Upsilon^a\right]\left[\Sigma^a\right]\left[V^a\right]^h \approx \begin{bmatrix} \bar{F}(j\omega_1) & \bar{F}(j\omega_2) & \cdots & \bar{F}(j\omega_q) \end{bmatrix} \tag{10}$$

where $[\Sigma^a] \in \mathbb{R}^{a \times a}$, $[V^a] \in \mathbb{C}^{q \times a}$, and $[\Upsilon^a] \in \mathbb{C}^{m \times a}$ are the singular values and basis vectors truncated to include only the significant singular values and associated singular vectors. By use of the modal transformation in (7), (10) may be restated in terms of physical forces as

$$\left[\Upsilon^a\right]\left[\Sigma^a\right]\left[V^a\right]^h \approx [U_{INPUT}]^T \begin{bmatrix} F(j\omega_1) & F(j\omega_2) & \cdots & F(j\omega_q) \end{bmatrix} \tag{11}$$

Projection of both sides of (11) onto the truncated basis $[\Upsilon^a]$ is performed as

$$\left(\left[\Upsilon^a\right]\left[\Upsilon^a\right]^\dagger\right)\left[\Upsilon^a\right]\left[\Sigma^a\right]\left[V^a\right]^h \approx \left(\left[\Upsilon^a\right]\left[\Upsilon^a\right]^\dagger\right)[U_{INPUT}]^T \begin{bmatrix} F(j\omega_1) & F(j\omega_2) & \cdots & F(j\omega_q) \end{bmatrix} \tag{12}$$

and reduces to

$$\left[\Upsilon^a\right]\left[\Sigma^a\right]\left[V^a\right]^h \approx \left(\left[\Upsilon^a\right]\left[\Upsilon^a\right]^\dagger\right)[U_{INPUT}]^T \begin{bmatrix} F(j\omega_1) & F(j\omega_2) & \cdots & F(j\omega_q) \end{bmatrix} \tag{13}$$

so that,

$$\left[U_{INPUT}\right]^T\begin{bmatrix} F(j\omega_1) & F(j\omega_2) & \cdots & F(j\omega_q) \end{bmatrix} \approx \left(\left[\Upsilon^a\right]\left[\Upsilon^a\right]^\dagger\right)\left[U_{INPUT}\right]^T\begin{bmatrix} F(j\omega_1) & F(j\omega_2) & \cdots & F(j\omega_q) \end{bmatrix} \quad (14)$$

Eq. (14) may be further simplified by placing restrictions upon the matrix of physical forces such that full row rank is assumed, allowing the application of a right inverse. To obtain full row rank, the physical force matrix must consist only of independent inputs, and the number of those inputs must be less than or equal to the number of spectral lines, q. Restriction to only independent inputs prevents consideration of cases where one or more forcing functions are distributed across multiple DOFs, which are beyond the scope of this work. Restriction on the total number of inputs is already incorporated in the prior assumption of $m \leq q$ for the singular value decomposition, when considered with the transformation of modal forces to physical forces. For (8) to provide a unique solution, the number of physical inputs considered in the pseudo-inverse must be less than or equal to the number of modes, m. Application of a right inverse to the physical force matrices of (14) yields

$$\left[U_{INPUT}\right]^T \approx \left(\left[\Upsilon^a\right]\left[\Upsilon^a\right]^\dagger\right)\left[U_{INPUT}\right]^T \quad (15)$$

which indicates that, for a set of input degrees of freedom to cause the estimated modal forces, the associated modal coefficients of the input degrees of freedom must be substantially similar to their projection onto the truncated basis $[\Upsilon^a]$. Consequently, a primary locator, *PL*, or localization function, may be constructed from the truncated basis and the mode shape coefficients of any set of N physical degrees of freedom. The value of the rth degree of freedom may be computed as

$$PL_r = \frac{\left|\left(\left[\Upsilon^a\right]\left[\Upsilon^a\right]^\dagger\left[U_r\right]^T\right)^h\left[U_r\right]^T\right|^2}{\left(\left(\left[\Upsilon^a\right]\left[\Upsilon^a\right]^\dagger\left[U_r\right]^T\right)^h\left[\Upsilon^a\right]\left[\Upsilon^a\right]^\dagger\left[U_r\right]^T\right)\left(\left[U_r\right]\left[U_r\right]^T\right)} \quad (16)$$

where $[U_r] \in \mathbb{R}^{1\times m}$ denotes the row of mode shape coefficients for the rth DOF over the m modes. The primary locator is a projection of the modal coefficients of each physical DOF onto the truncated basis described by $[\Upsilon^a]$. When the modal coefficient vector of a DOF exists within the space described by $[\Upsilon^a]$, that DOF is compatible with the modal forces, such that a force applied at that associated location is capable of providing some or all of the modal force required to cause the observed response, without causing additional unrelated forces. Projection of the coefficient vector for a compatible DOF onto the truncated basis will cause minimal change to the modal coefficient vector, such that evaluation of (16) will produce a high value. Application of a force at an incompatible DOF will produce an unrelated modal force pattern. Projection of the modal coefficients of an incompatible DOF onto the truncated basis will yield changes in the coefficient vector and result in a lower value of the primary locator. The function outputs values from 0 to 1 and may be used for any number of physical degrees of freedom available from a set of augmented mode shapes, regardless of sensor placement. Figure 1 provides a conceptual representation of the localization process, starting with the composition of m modal forces from N physical inputs over q spectral lines, proceeding through the SVD to determine the truncated basis and ending with the representation of the primary locator function for a number of a degrees of freedom.

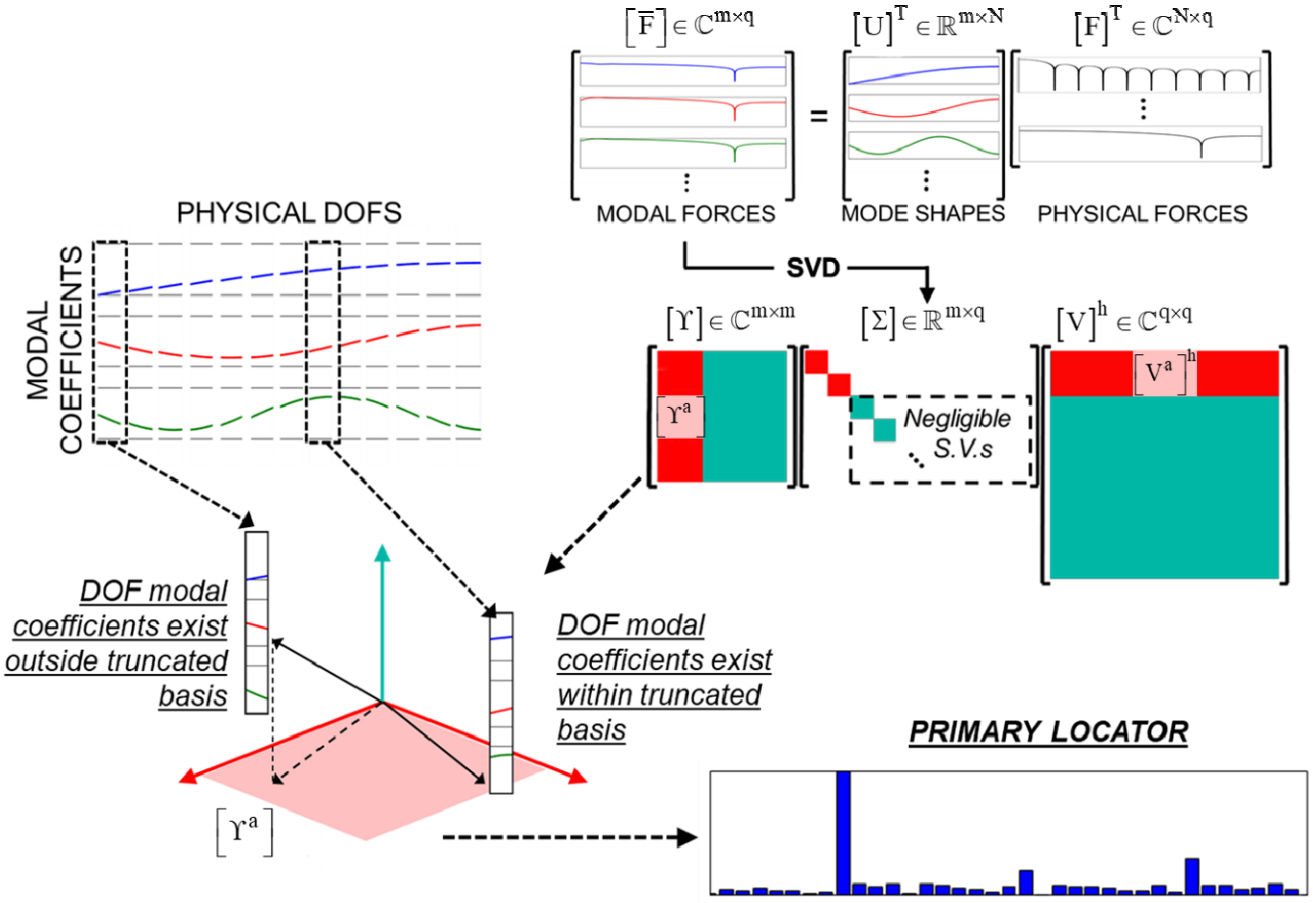

Figure 1. Modal forces, synthesized from physical inputs and modal coefficients, may be decomposed to determine the number of independent sources and the associated truncated sets of singular vectors, which may be used to develop a locator function using the modal coefficients of any number of degrees of freedom.

Figure 2 depicts the larger input identification process starting from physical responses caused by an unknown input and ending at an identified input. Physical responses are transformed to modal responses, from which modal forces are estimated. The singular value decomposition is performed and truncated bases are identified, as illustrated in Figure 1. The primary locator function, (16) is applied to locate potential compatible DOFs. Once input locations are determined, physical force may be estimated by projection of the modal force back to physical space.

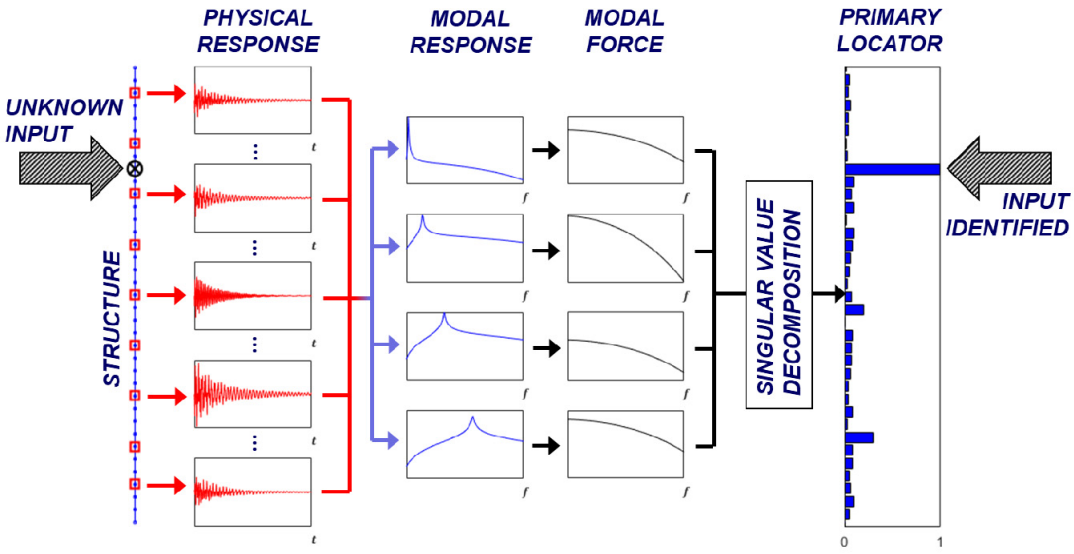

Figure 2. Process for input identification from responses caused by an unknown input.

SYSTEM DESCRIPTION

To provide validation, force reconstruction was applied to a lab structure consisting of three aluminum plates: a base plate, an upright plate, and a wing-like plate bolted to the upright plate. The plate dimensions are 60.96 cm by 60.96 cm by 1.9 cm (24 in by 24 in by 0.75 in) for the base plate, 76.2 cm by 60.96 cm by 1.9 cm (30 in by 24 in by 0.75 in) for the upright plate and 60.96 cm by 60.96 cm by 1.27 cm (24 in by 24 in by 0.5 in) for the wing. A finite element model of the structure was created to determine sensor locations and to permit subsequent localization via (16). The model consisted of 39168 plate elements, with angle brackets represented by an additional 4224 solid elements and 1552 rigid elements to join the components. The mesh resolution afforded a node spacing of 6.35 mm (0.25 in). Ten triaxial accelerometers and 24 uniaxial accelerometers were used for response measurements. Sensor selection and placement was performed to best distinguish the modes of interest. The structure, model and test grid are shown in Figure 3. Modal analysis was performed via impact hammer, with the resulting correlation between model and test provided in Table 1.

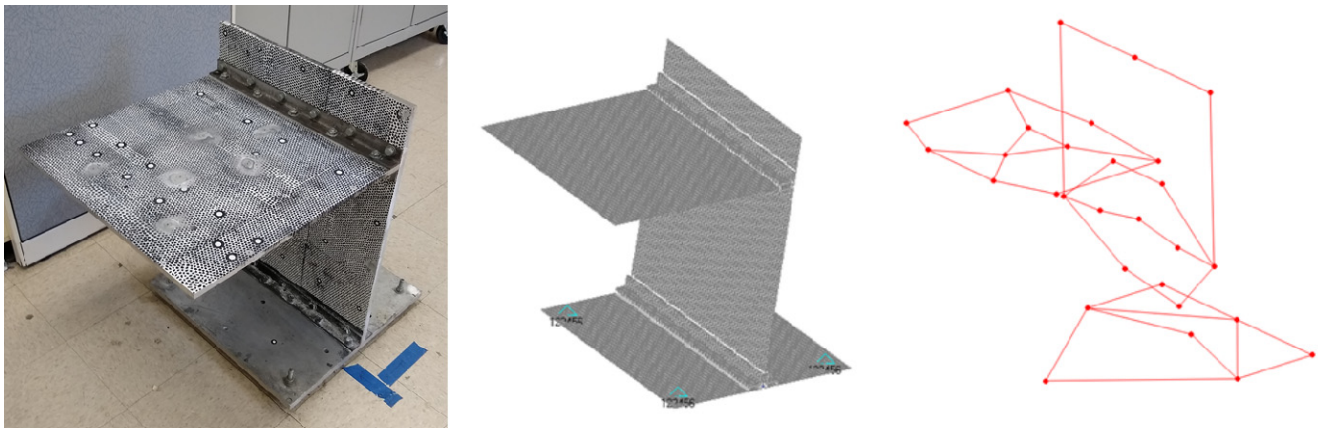

Figure 3. Test structure (left), finite element model (center) and test grid (right).

Table 1. Correlation for finite element modes (FEA) vs test modes (EMA).

Mode	Frequency (Hz) FEA	EMA	Diff. (%)	MAC	Mode	Frequency (Hz) FEA	EMA	Diff. (%)	MAC
1	14.3	13.9	2.84	99.8	13	431	422	2.18	98.8
2	30.6	29.4	4.18	99.4	14	458	459	-0.29	93.9
3	33.4	32.4	2.98	99.3	15	462	464	-0.35	93.3
4	56.1	51.9	7.94	98.5	16	530	535	-0.85	82.3
5	75.1	74.9	0.26	98.7	17	549	541	1.53	75.1
6	100	91.5	9.64	98.5	18	574	595	-3.48	70.4
7	150	149	0.44	98.6	19	608	598	1.77	89.1
8	217	218	-0.38	91.1	20	699	688	1.58	92.8
9	243	240	1.28	88.8	21	776	763	1.72	95
10	255	251	1.75	95.5	22	785	796	-1.37	93.6
11	318	305	4.37	96.2	23	829	823	0.76	95.9
12	361	354	1.98	98.3	24	853	839	1.64	90.3

A force gage with a soft plastic hammer tip attached was placed in contact with the wing along the free edge of the wing, located at x = -61.3 cm, y = 53.3 cm. The hammer tip acted as a thumper (nonlinear contact), such that structural response would cause intermittent contact between the structure and the hammer tip, with the force gage used to measure contact forces for comparison. The thumper is shown in Figure 4.

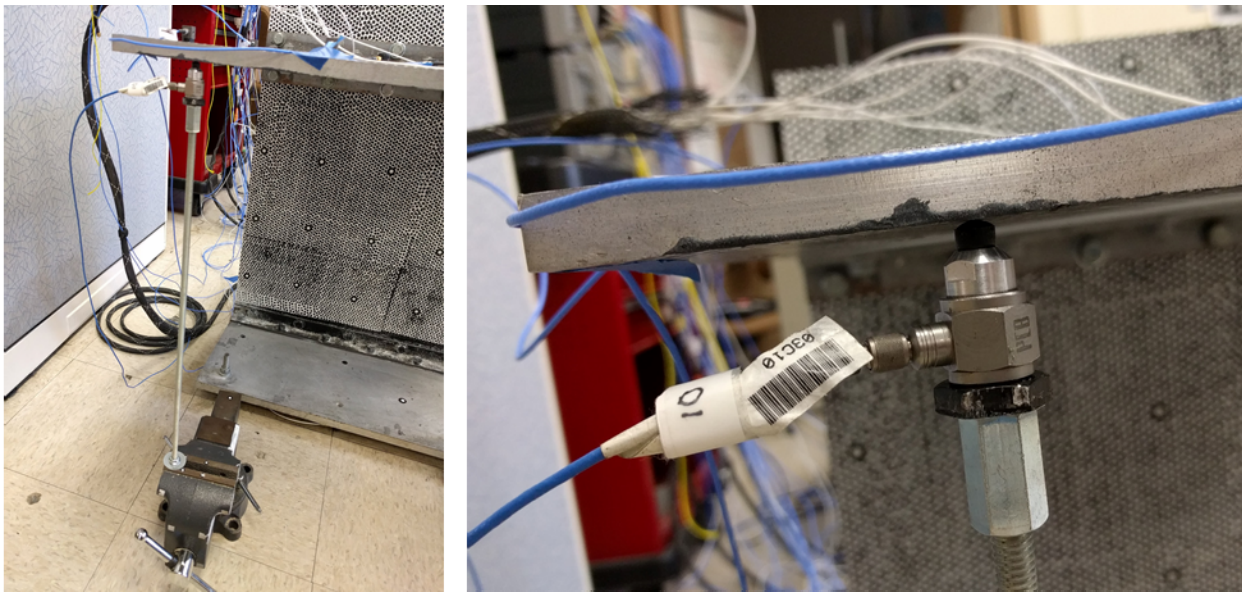

Figure 4. Thumper located under wing (left), with close up of thumper (right).

EXPERIMENTAL FORCE RECONSTRUCTION WITH NONLINEAR GAP CONTACT

With the thumper in place, an impact was applied on the upright plate, at y = 7.6 cm, z = 66.0 cm. Response data was collected over an 8 s sample interval, at 4096 samples/s. Modal responses were estimated from the physical responses via (5), using the experimental mode shapes as the basis for the modal filters. Responses from modes 1-5, 7-11, 13 and 16 were used for estimation of modal forces via (6). The remainder of the modes were excluded from the estimation process because they did not participate significantly in the response and were largely characterized by noise. Additionally, the frequency content above 500 Hz indicated high levels of noise contamination, relative to the actual response, across the modes. The frequency content below 100 Hz indicated high levels of noise for the higher modes used, but not the lower modes. To mitigate the effects of the contaminants, singular value decomposition was performed using the modal forces over the 100 Hz to 500 Hz band. The SVD indicated that the first two singular values represented over 99% of the estimated modal forces. The primary locator function was computed for the three plates using the first two singular vectors. Figure 5 shows the singular values and the localization functions for the wing, upright and base plates.

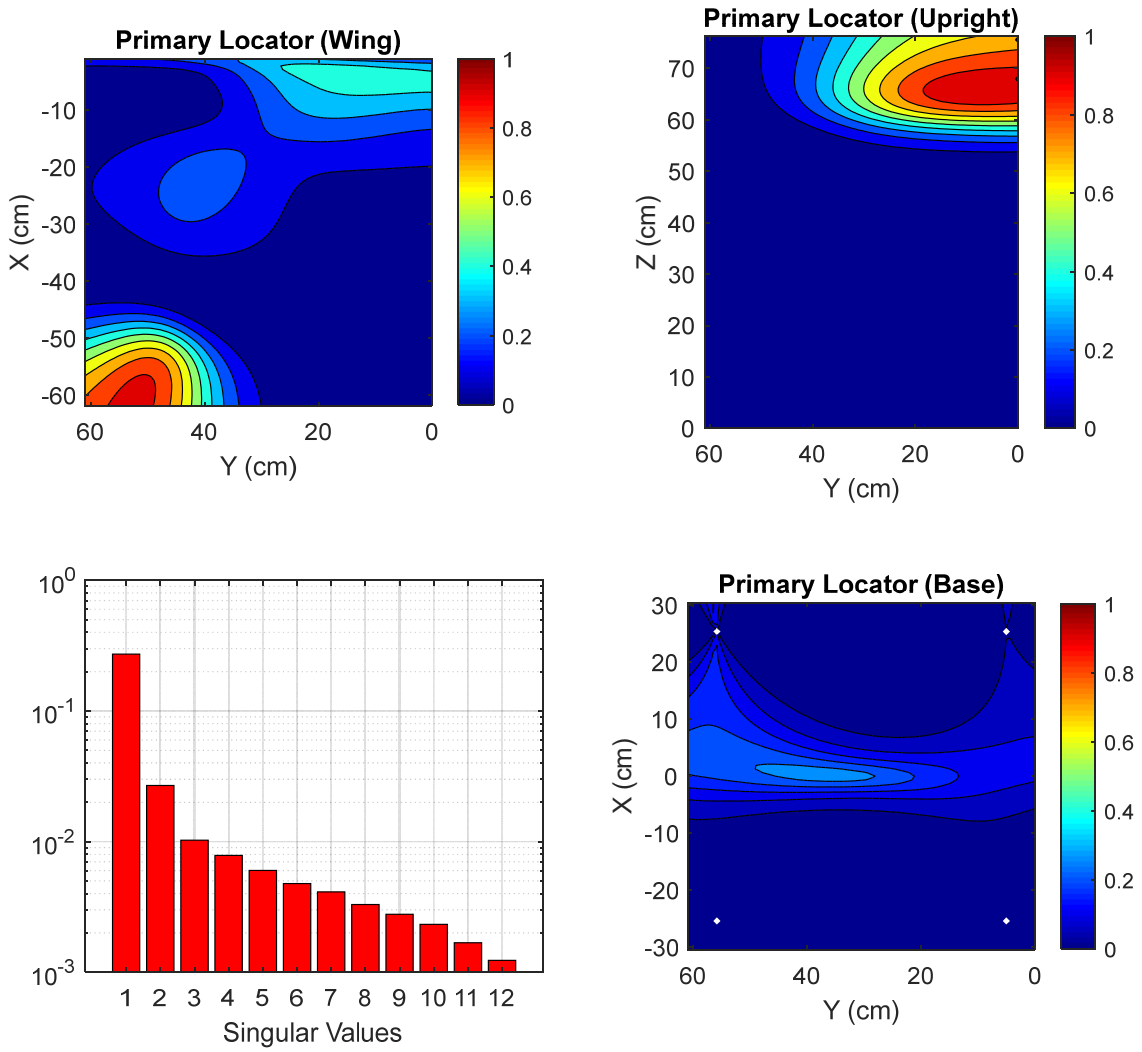

Figure 5. Singular values (bottom left) from the modal forces, with localization functions for the wing (top left), upright (top right) and base plate (bottom right).

The locator functions for the wing and upright both indicate the presence of some force. For the upright plate, force is indicated at y = 5.7 cm, z = 66.0 cm. When compared with the actual hammer impact location of y = 7.6 cm, z = 66.0 cm, and considering the plate diagonal as the characteristic length of the plate, the input has been located to within 2% of the characteristic length. For the wing, force is indicated at x = -61.9 cm, y = 52.7 cm. When compared with the thumper location of x = -61.3 cm, y = 53.3 cm, the thumper has been located to within 1% of the characteristic length of the wing.

Note that neither the hammer input nor the contact forces were collocated with an accelerometer. The estimated physical modal forces were projected to physical space via (8), using the finite element modal coefficients of the identified input locations. The estimated modal forces for modes 1-3 were used to reconstruct the physical forces over the 10 Hz to 100 Hz band, supplementing the 100 Hz to 500 Hz content across the larger mode set. The frequency domain estimates for the hammer input and contact were returned to the time domain via IFFT, and are shown in Figure 6.

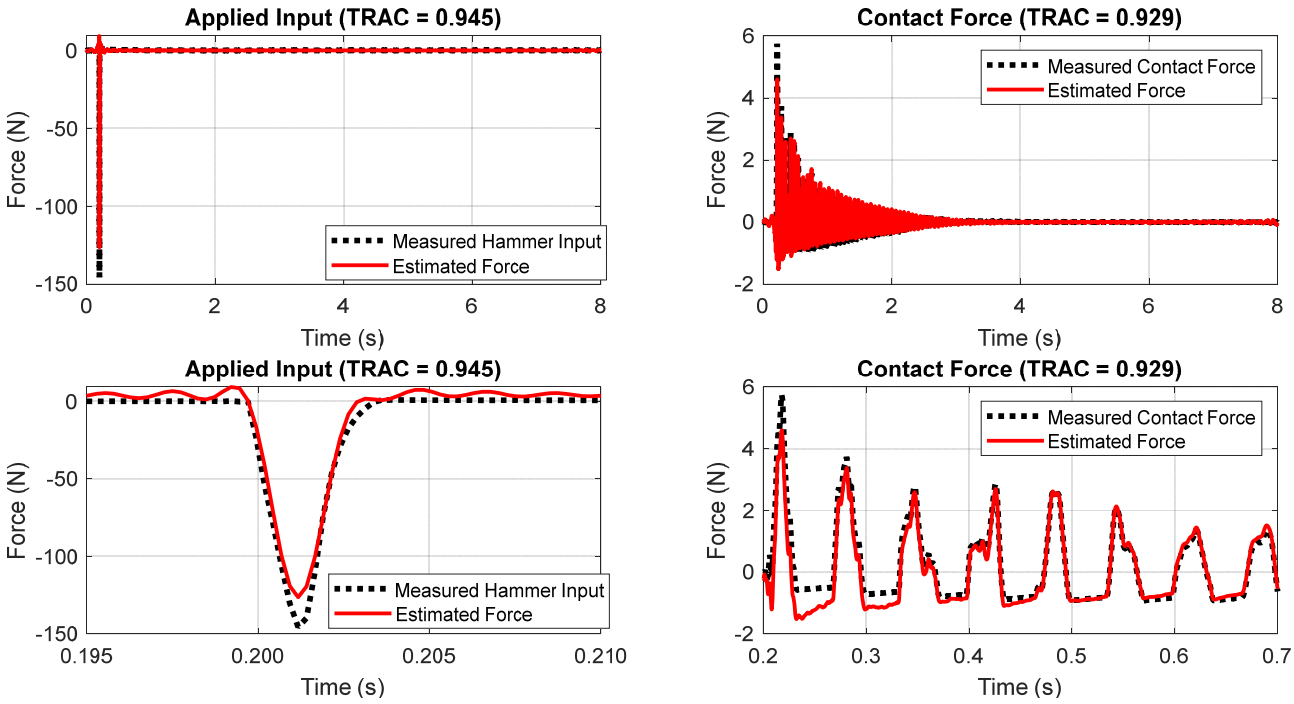

Figure 6. Estimated and measured hammer input over the sample interval (top left), focused comparison of hammer input pulse and estimate (bottom left), contact forces and estimate over the sample interval (top right) and focused comparison of the contact forces and estimate (bottom right).

Visually, the estimates compare well with the measured forces. The estimate of the hammer input shows a maximum amplitude of 126.3 N, compared with the measured maximum amplitude of 145.5 N, for a difference of approximately 15%. The maximum measured contact force is 5.74 N, while the maximum estimated contact force is 4.6 N, for a difference of approximately 20%. The TRAC for the estimated and measured hammer pulses is 94.5%, while the TRAC for the estimated and measured contact forces is 92.9%. Both TRAC values indicate very good correlation between the estimated and measured forces, despite the differences in maximum magnitude. However, as demonstrated in the analytical case, the estimates for the experimental validation only contained frequency content from 10 Hz to 500 Hz, and appear to be affected by frequency content truncation.

To confirm the effects of the truncation, frequency content below 10 Hz and above 500 Hz was removed from the measured forces for further comparison with the estimates. Overlays of the estimates with the reference measurements, as well as the truncated reference measurements, are shown in Figure 7. With truncation of the measured forces, the maximum amplitude of the hammer pulse changed from 145.5 N to 134.3 N, for a difference of approximately 6% from the estimated maximum value of 126.3 N. The maximum contact force changed from 5.74 N to 4.82 N, for a difference of approximately 5% from the estimated maximum value of 4.6 N. Additionally, the TRAC was recomputed for the estimates and the frequency-truncated measurements, with the correlation values above 99.5% in both cases. By examining the estimated and measured forces based only on consistent frequency content, the agreement between the estimates and the measurements appears to be very good.

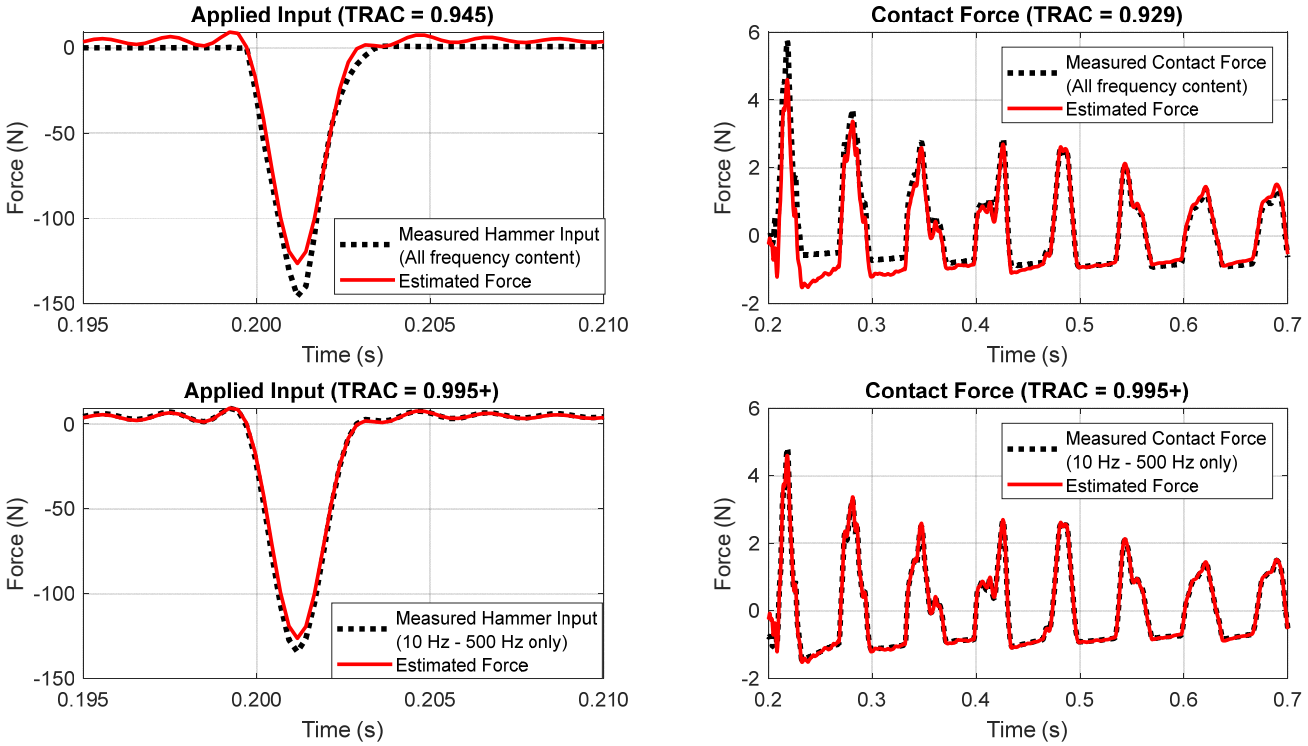

Figure 7. Estimated hammer pulse and measured pulse with all frequency content (top left) and 10 Hz to 500 Hz content only (bottom left), as well as estimated contact force and measured contact force with all frequency content (top right) and 10 Hz to 500 HZ content only (bottom right).

CONCLUSION

A force reconstruction technique has been applied to the characterization of nonlinear gap contact. Use of a limited set of sensors allowed for localization and characterization of external loads as well as contact forces. While the methodology has previously been demonstrated analytically as capable of characterizing certain nonlinearities through their equivalent loading, this work provided experimental validation. Forces were located to within 2% of the characteristic length of the affected components. Although some differences existed between the estimated forces and the measured forces, the differences were largely attributable to frequency content truncation in the estimates. By comparing only like frequency content, the maximum amplitudes of the estimates were determined to differ by no greater than 6% from the measured forces. Additionally, the correlations between the estimates and the measured forces were very good, with correlation values greater than 99%. Future work shall examine data rejection criteria as an alternative to manual data selection

ACKNOWLEDGEMENTS

Some of the work presented herein was partially funded by Air Force Research Laboratory Award FA8651-16-2-0006 “Nonstationary System State Identification Using Complex Polynomial Representations” as well as by NSF Civil, Mechanical and Manufacturing Innovation (CMMI) Grant No. 1266019 entitled “Collaborative Research: Enabling Non-contact Structural Dynamic Identification with Focused Ultrasound Radiation Force”. Any opinions, findings, and conclusions or recommendations expressed in this material are those of the authors and do not necessarily reflect the views of the particular funding agency. The authors are grateful for the support obtained.

REFERENCES

1. Farrar, C.R., Doebling, S.W.: An overview of modal-based damage identification methods. In: Proceedings of DAMAS conference 1997, pp. 269-278. Citeseer
2. Das, S., Saha, P., Patro, S.: Vibration-based damage detection techniques used for health monitoring of structures: a review. Journal of Civil Structural Health Monitoring **6**(3), 477-507 (2016).
3. Gunes, B., Gunes, O.: Structural health monitoring and damage assessment Part I: A critical review of approaches and methods. International Journal of Physical Sciences **8**(34), 1694-1702 (2013).
4. Fan, W., Qiao, P.: Vibration-based damage identification methods: a review and comparative study. Structural health monitoring **10**(1), 83-111 (2011).
5. Zhang, Q., Allemang, R., Brown, D.: Modal filter: Concept and applications. Paper presented at the 8th International Modal Analysis Conference, Kissimmee, FL, USA,
6. Logan, P., Avitabile, P.: Impact Reconstruction Using Modal Filters. Paper presented at the 36th International Modal Analysis Conference, Orlando, FL,
7. Logan, P., Fowler, D., Avitabile, P.: Validation of Force Reconstruction for Linear and Nonlinear System Response. Paper presented at the 37th International Modal Analysis Conference, Orlando, FL,